

A Dynamic, Hierarchical Resource Model for Converged Computing

Daniel J. Milroy

Lawrence Livermore National Laboratory
Livermore, CA, USA
milroy1@llnl.gov

Stephen Herbein

Lawrence Livermore National Laboratory
Livermore, CA, USA
herbein1@llnl.gov

Claudia Misale

IBM T. J. Watson Research Center
Yorktown Heights, NY, USA
c.misale@ibm.com

Dong H. Ahn

Lawrence Livermore National Laboratory
Livermore, CA, USA
ahn1@llnl.gov

ABSTRACT

Extreme dynamic heterogeneity in high performance computing systems and the convergence of traditional HPC with new simulation, analysis, and data science approaches impose increasingly more complex requirements on resource and job management software (RJMS). However, there is a paucity of RJMS techniques that can solve key technical challenges associated with those new requirements, particularly when they are coupled. In this paper, we propose a novel dynamic and multi-level resource model approach to address three key well-known challenges individually and in combination: i.e., 1) RJMS dynamism to facilitate job and workflow adaptability, 2) integration of specialized external resources (e.g. user-centric cloud bursting), and 3) scheduling cloud orchestration framework tasks. The core idea is to combine a dynamic directed graph resource model with fully hierarchical scheduling to provide a unified solution to all three key challenges. Our empirical and analytical evaluations of the solution using our prototype extension to Fluxion, a production hierarchical graph-based scheduler, suggest that our unified solution can significantly improve flexibility, performance and scalability across all three problems in comparison to limited traditional approaches.

KEYWORDS

converged computing; dynamic heterogeneity; resource subgraph inclusion

1 INTRODUCTION

The demise of Dennard scaling in the early 2000s spurred high performance computing (HPC) to embrace parallelism and rely on Moore’s law for continued performance improvement. HPC now finds itself near the end of Moore’s law. The end of the two trends has resulted in exponentially increasing parallelism and the adoption of accelerators (GPUs, field programmable gate arrays, and other specialized technologies), leading to “extreme heterogeneity” and “dynamic heterogeneity” in system resources [24]. Furthermore, the increasing integration of cloud computing with HPC allows applications on-demand access to pools of external resources that can change over time depending on their cost or availability. State-of-the-art supercomputers feature extreme and dynamic heterogeneity and incorporate cloud technologies, forming highly complex and

dynamic systems [3, 4, 23]. Exascale systems are expected to further the trend to a greater scale and integrate cloud resources seamlessly.

Cutting-edge scientific workflows are coevolving and becoming far more complex, often integrating machine learning and visualization with multiscale or multiphysics models. The added sophistication derives from a need to solve large, interdisciplinary problems such as automating lead optimization in drug discovery [25], understanding protein interactions with cell membranes for cancer research [10], and responding to global crises like the COVID-19 pandemic by accelerating drug design [17]. According to the United States Department of Energy, increasingly complex “workflows will need to adapt on-the-fly to rapidly changing resource, data, and user constraints” and require resource management and scheduling adaptability to “match the dynamically changing resource requirements of a job, as well as the changing performance and availability of the resources themselves” and in turn alter scheduling decisions in “response to unfolding events such as new data, changes to [a] workflow, or changes in cost or availability of resources” [24].

There are three well-known key technical challenges one must solve to address extreme and dynamic heterogeneity: 1) RJMS dynamism to facilitate job and workflow adaptability, 2) integration of specialized external resources (e.g. user-centric cloud bursting), and 3) scheduling elastic cloud orchestration framework tasks. While each of these challenges is unique and individual solutions to each challenge do exist (e.g. [2, 6, 21]), we argue that these challenges must be viewed as “interrelated”: i.e., they are expected to be increasingly combined as HPC and cloud environments become more tightly converged. However, there is a dearth of work on techniques that consider and address all three core problems combined.

We observe that a lack of more effective resource data models commonly underlies these problems. Extreme heterogeneity and resource dynamism produce an explosive growth in the space of configurations that can be requested by a job. The rapid growth of the resource configuration space exposes limitations of existing RJMS. Current resource data models are often based on simplistic, rigid representation schemes, which may also be static, requiring that new resource types and relationships be defined in a configuration file. Static representations are ill-suited to satisfying requests for dynamic and external (e.g. cloud) resources, and limit the ability to integrate resources returned from a cloud provider based on specification of cost or location rather than hardware.

We propose novel distributed graph-based techniques as a dynamic, fully hierarchical resource model to solve all three challenges individually and in combination. The primitive operations of our solution are adding or removing a target resource subgraph from an existing resource allocation or system. Our solution includes a novel technique that ensures scalability by adding or removing a subgraph without updating the entire graph state, which can be distributed across a hierarchy of scheduler instances. Our approach is formulated in the context of fully hierarchical scheduling, one of the most general forms of HPC scheduling. We adapt fully hierarchical scheduling to integrate externally provided resources (e.g., cloud resources) selected and returned by the external provider, and enable specialization of the provider itself. Our unique strategy of combining fully hierarchical scheduling with a dynamic graph-based resource model provides the flexibility and efficiency to manage massive resource configuration spaces.

Specifically, we make the following contributions:

- the notion of resource subgraph inclusion partial ordering within fully hierarchical scheduling which allows us to define resource graph transformations (e.g., adding a new vertex or edge) and external resource specialization;
- embodiment of simple hierarchical and distributed algorithms for resource dynamism by extending Fluxion[15], a production graph-based scheduler;
- suitability of our solution for local and external resource addition by testing its performance on a local cluster, with HPC+AWS and on a converged HPC and cloud environment by extending KubeFlux (Kubernetes integrated with Fluxion) with elasticity, and performing an analytical analysis of the hierarchical algorithms.

Our studies reveal that there is minimal memory and runtime overhead associated with resource addition of local and external cloud resource for single-level jobs, and indicate that our methods are efficient for multi-level jobs.

2 CURRENT EFFORTS TO MANAGE DYNAMIC HETEROGENEITY

Complex workflows such as the Multiscale Machine-Learned Modeling Infrastructure (MuMMI) [10], Accelerating Therapeutics Opportunities in Medicine Modeling Pipeline (AMPL) [17], and Clustered Atom Subtypes aidEd Lead Optimization (CASTELO) [25] represent directions of future workflow development and feature several techniques that depend on resource dynamism and heterogeneity. In particular, MuMMI and AMPL contain stages with many independent tasks, known as ensembles, which are becoming increasingly prevalent in HPC. AMPL and CASTELO also rely on external resources in the form of on-premises cloud technologies. In this Section, we explore current work on resource dynamism and limitations and challenges.

2.1 Ensemble-based workflows and elasticity

Ensemble jobs constitute as many as 48% of the jobs run on a large cluster sited at Lawrence Livermore National Laboratory (LLNL), one of the world largest supercomputing centers, and can severely tax the capabilities of centralized schedulers on near-exascale machines [7]. Large centers like LLNL use fully hierarchical scheduling

to tackle the scalability limitations of centralized schedulers. In fully hierarchical scheduling, any scheduler instance can spawn child instances to aid in scheduling, launching, and managing jobs, which can recurse to an arbitrary depth. While fully hierarchical scheduling has proven effective in overcoming scheduling bottlenecks [7], researchers at LLNL discovered that for those ensemble workflows that change resource requirements at runtime, an inability to resize resource shapes at lower level schedulers can still lead to resource underutilization or limit performance.

Jobs or workflow components that change shape through adding more resources, relinquishing resources, or allowing their allocations to be altered by the scheduler can increase efficiency and throughput [12, 14, 21]. Jobs capable of one or more of these types of dynamism are called adaptive jobs [11]; the Slurm scheduler [26] supports adaptive jobs by allowing a running job to submit a new job with a dependency indicator and then merging the allocations. However, the approach used by Slurm demands that an adaptive job release all the nodes that came with a single dynamic request. Hereafter we use “elastic jobs” to designate adaptive jobs that can “burst” to cloud or other external resources.

2.2 Converged computing and cloud bursting

Bringing the best features of HPC and cloud together in a converged environment is of considerable interest to both communities. Containers offer significant advantages to traditional applications in terms of reproducibility and portability, which are attractive to the HPC and data science communities. Kubernetes is the de facto container orchestrator, and it is widely used for running cloud-native applications ranging from traditional microservices to AI workflows. Kubernetes is highly customizable, and it can be extended to introduce new capabilities. HPC RJMS provide sophisticated scheduling based on desired application placement and shape such as fine-grained hardware requirements, job co-scheduling, easy specification of affinity, or group/gang scheduling. Kubernetes’ default scheduler does not provide these features, so the orchestration community is responding to address these limitations by creating new plugins such as NUMA aware container placement¹. IBM and LLNL’s approach the problem through a collaboration to integrate Fluxion into Kubernetes. Specifically, the IBM-LLNL KubeFlux project implements a plugin scheduler for Kubernetes using Fluxion. To create a job allocation, KubeFlux invokes Fluxion’s resource-query tool with a Fluxion job specification that includes an encoded Kubernetes pod specification. While this addresses the aforementioned HPC scheduling problems within the cloud, KubeFlux lacks the ability to grow or shrink a resource allocation. Similarly to typical Kubernetes workflows, users running scientific workflows under KubeFlux want the capability to grow an allocation and spawn more containers as needed for some phases or to shrink the allocation during others. A lack of elasticity within current HPC RJMS leads to a technology mismatch that prevents seamless convergence between HPC and cloud computing.

A popular form of HPC and cloud convergence is cloud bursting, where an application running on an HPC system extends its execution environment into a cloud. Bursting allows applications to consume additional resources if no satisfactory resources are

¹<https://kubernetes.io/docs/tasks/administer-cluster/topology-manager/>

available in the local HPC cluster. While a hybrid HPC-cloud environment can outperform either of its components, care must be taken to identify applications which can benefit from bursting [13]. Much work has been done studying application suitability for cloud execution and bursting, which has concluded that network performance is a primary bottleneck, impacting tightly-coupled applications in particular [18]. However, more loosely-coupled and high-throughput applications (or steps for a composite application) are suitable for cloud environments [18].

Several production HPC schedulers such as Slurm [26], PBS Pro [8], and Spectrum LSF [2] support bursting into the cloud with elastically-provisioned resources. They provide policies defining when to burst into and relinquish resources from the cloud and limit the maximum number of cloud resources to use at any time. However, Slurm and PBS Pro possess significant limitations to their bursting capabilities.

Slurm and PBS Pro base their resource data models on simplistic, rigid representation schemes such as bitmaps. A bitmap is a rigid representation of a set of homogeneous compute nodes and their states where each bit represents whether a node is allocated or free. While bitmaps are highly optimized for rigid HPC resources and workflows (e.g., using a few bitwise operators to find idle nodes), the need for global updates to each dynamic resource expression and difficulties in handling diverse resources make this approach increasingly confining.

Slurm and PBS Pro define resources and their attributes via static configuration. As a result, the cloud instance types must be chosen by the user a priori, either by selecting a queue tied to a particular type or by providing a command line argument specifying the instance types. We hypothesize that such limitations often arise from the rigid resource models used in the traditional approach. These limitations not only include difficulties with static configurations but also performance variabilities when they do not consider performance-critical constraints for the elastic resources (e.g., the hosts must be scheduled from a specific number of zones and racks).

Spectrum LSF is far more flexible in that it can integrate cloud resources that are chosen by the cloud provider to meet requests based on location or cost. However, it also suffers from limitations derived from static mappings. Enabling or reconfiguring users for bursting to cloud providers is achieved via a static, cluster-wide configuration. LSF does not currently support user-centric external resource specialization.

3 SCALABLE GRAPH EDITING TECHNIQUES FOR ELASTICITY

Directed graph resource models and fully hierarchical scheduling are powerful tools, but in combination they address the significant challenges we identify in Section 1 of managing extreme, dynamic heterogeneous configuration spaces. In this section we define our core approach through a subgraph partial ordering and primitives for addition and removal of resources within fully hierarchical scheduling. Graphical fully hierarchical scheduling is one of the most general ways to address HPC and cloud convergence and elastic jobs since the distinction between external and local resources is recast as a parent and child relationship. In the discussion that

follows we assume the scheduling hierarchy is a tree. In the context of fully hierarchical scheduling, we refer to the initial hierarchical scheduling instance as the top-level scheduler and its resource graph as G_0 . Note that any child instance of the multi-level scheduler will instantiate a resource graph that is a subgraph of G_0 . More generally, for any child instance resource graph G_c of a parent instance resource graph G_p : $G_c \subseteq G_p$. To reduce memory usage, each instance initializes its resource graph with only those resources within its purview. As a simple example, for a cluster of three nodes, an instance that has requested and received two nodes from the top level will instantiate its resource graph with only those two nodes. The child has no knowledge of resources outside of its graph. For a general nested job of n levels with each level starting a different number of child jobs $j = (a_1, a_2, \dots, a_k)$, we have a sequence of sequences of jobs $(j_i)_{i=1}^n$. If each child starts exactly one job, we have the following sequence of resource subgraph partial orderings:

$$G_0 \supseteq G_1 \supseteq G_{1_1} \supseteq \dots \supseteq G_{1_1 \dots 1_1} \quad (1)$$

$\underbrace{\dots}_n$
n-times

Now a dynamic resource subgraph is any resource subgraph that can change its topology. A typical example is to add a new vertex and edge. There are several implications to consider.

First, subjecting any subgraph in the sequence to a nontrivial topology transformation invalidates the subgraph inclusion sequence. In particular, if some graph transformation T is applied to any subgraph in the inclusion sequence, the entire sequence can be invalidated. More formally, a general T which adds new and deletes existing vertices and edges invalidates the entire inclusion sequence:

$$G_0 \not\supseteq G_1 \not\supseteq T(G_{1_1}) \not\supseteq \dots \quad (2)$$

Second, a transformation that only adds vertices and edges invalidates the supergraph inclusion subsequence, while a transformation that only deletes vertices and edges invalidates the subgraph inclusion subsequence. The invalidation “direction” imposes a natural direction of application for the transformation operation T . Therefore an additive transformation naturally proceeds from the top down, while a subtractive transformation moves from the bottom up. Third, in order to add vertices to subgraph n , the vertices must be added to the $n - 1$ supergraphs. The addition is the identity if the vertices already exist in any supergraph. A similar argument can be applied to the removal of vertices or edges. Fourth, which vertices and edges must be added are predicated on finding resources *matching* a resource request.

External resource specialization, or the ability for each user to choose the external resource providers of their preference is related to the subgraph partial order of graphical fully hierarchical scheduling. For external resource specialization we allow the additive transformation to invalidate the supergraph inclusion sequence. In other words, external resources E_i are managed by a first-level allocation G_i independent of the top-level scheduler. Independent management of external resources cannot create allocation inconsistencies since $G_i \setminus G_0 = E_i$. Independent management enables consistent resource management for bursting to external resources

as well as full flexibility for specializing the external provider. However, if a site requires that external resources are available for any user the addition transformation can be configured not to invalidate the supergraph inclusion sequence. Graph-based fully hierarchical scheduling is naturally suited for pairwise parent-child communications between levels. The modular parent-child structure enables a simple recursive strategy for communicating subgraph changes. Resource transformations are communicated up or down the subgraph sequence, and are prompted by a resource match request specification referred to as a jobspec. The procedure to match available resources to a jobspec and allocate them upon a successful match is `MATCHALLOCATE(MA)`. `MATCHGROW(MG)` attempts to match available resources to a jobspec in the local subgraph, but forwards the request to its parent if the match fails. See Algorithm 1 for details.

In the following discussion we assume that a leaf scheduler instance makes a request for additional resources, but any nested level can initiate a request. To add resources to a leaf instance, the leaf issues a `MG`, passing a jobspec as an argument. If satisfactory resources are located within the leaf's resource graph, the resource graph scheduling metadata is updated to indicate that new resources are now attached to the job. A successful single-level `MG` behaves almost identically to the standard `MA`; the difference is that the new resources are given the allocation metadata of a running job allocation. If resources are not found locally, the leaf issues a `MG` to its parent. If the new resource request cannot be met, the parent issues the same job request to its parent and so on up the tree via `MG` recursion. When matching resources are found, the scheduling metadata is updated and the new subgraph is sent to the child. The child adds the new vertices and edges into its resource graph and updates its scheduling metadata. The top-down process proceeds until reaching the originating leaf. We refrain from discussing procedures for removing resources from the subgraph inclusion sequence since they are analogous to `MG`.

To be scalable, it is important to limit the requisite updates to the minimum set of vertices and edges in these procedures. Thus, we use a technique called *localization* as we only perform local updates in these procedures. Assuming the graph implementation indexes vertices by their graph paths, which holds true for the Fluxion implementation of fully-hierarchical scheduling, we can use the index to locate the attaching point of the subgraph in constant time. This makes the computational complexity of `ADDSUBGRAPH` $O(n + m)$ for a subgraph of n vertices and m edges. Further, the metadata within each vertex is organized such that each vertex will only contain the metadata about itself and certain quantities as a function of its subgraph (e.g., subtree rooted at that vertex). Thus, attaching a new subgraph only requires updating its ancestor vertices. This limits the computational complexity of `UPDATEMETADATA` to be $O(n + m + p)$ for a subgraph of n vertices and m edges with p supergraph ancestors.

We provide an `EXTERNALAPI` to translate additive or subtractive transformations from the hierarchical scheduler into external resource provider functions. The `EXTERNALAPI` takes a jobspec as an argument, and translates the specification to a request for external resources, calling the provider API to create or start instances. The API returns the resources as a subgraph, so the remainder of the `MG` process can proceed as if the resources originate from a local

parent. To a scheduler instance, the external resource provider is functionally just another parent in the hierarchical scheduling.

4 ENABLING ELASTICITY IN FLUXION

In this section we describe our implementation of the procedures described in Section 3 in Fluxion to enable elasticity and management of extreme, dynamic heterogeneity. We also discuss how enabling elasticity in Fluxion allows cloud computing technology like KubeFlux to grow or shrink resource allocations.

The Fluxion resource graph relies on Boost Graph Library (BGL) [1] to provide the underlying directed graph data structure. We use vertex and edge addition and removal functions provided by BGL to transform the resource graph. Subgraphs to be added or removed are encoded in JSON Graph Format (JGF) which can then be transmitted between parent and child schedulers via Remote Procedure Call (RPC) functionality built into the Flux RJMS framework [7]. For example, if a child issues `MATCHGROW` via RPC to its parent and the match is successful, the matching resources are returned in JGF as part of the call.

To add and remove resources from an external provider, we implement `EXTERNALAPI` from Section 3 with the popular AWS API. The AWS API is extremely rich and configurable, making it an ideal API for use with Fluxion. We use the Python (boto3) AWS API as it is well-documented and suitable for rapid integration prototyping in Fluxion. Our implementation (`EC2API`) takes a Fluxion jobspec as an input argument, and depending on the jobspec either maps the request to corresponding EC2 instance types or builds an EC2 Fleet request for generic resources. Then `EC2API` makes the AWS API call to create the resources and returns the new subgraph in JGF to Fluxion. One of the powerful capabilities afforded by a directed graph representation of resources is the inclusion of the physical location of the resources. `EC2API` can interpose an EC2 zone vertex between the nodes' vertices and the cluster vertex. Location information allows the application to make location-dependent decisions which can be particularly important for using cheap AWS spot instances or reliably storing data in multiple S3 zones.

5 EXPERIMENTAL WORK

In this section we conduct a series of experiments to test whether Fluxion, a graph-based fully hierarchical scheduler, can effectively provide the three capabilities identified in Section 1 as necessary for managing extreme, dynamic heterogeneity. First, we investigate the performance of additive graph transformation in the context of a traditional adaptive HPC task. Second, we test Fluxion's performance for scheduling elastic Kubernetes tasks with KubeFlux. Finally, we examine Fluxion's `EXTERNALAPI` performance by integrating AWS cloud resources, and compare its flexibility to that of Slurm and Spectrum LSF through managing EC2 Fleet resources. The experiments in this section test the three primary components of resource graph growth: the time to find new resources, the time to communicate new resources in the form of a subgraph, and the time needed to add the new subgraph into the existing resource graph and update its state.

We test Fluxion on two nodes of a dedicated test cluster at LLNL. Each node features dual-socket Intel Xeon E5-2660 CPUs with 16 cores and 64 GB memory; internode communications are performed

Algorithm 1 Bottom-up then top-down MatchGrow procedure

```

1: function ADDSUBGRAPH(subGraph)
2:   graph ← GETGRAPH()
3:   for (sourceVertex, targetVertex) in subGraph.edges do
4:     if sourceVertex and targetVertex in graph.vertices then
5:       if (sourceVertex, targetVertex) not in graph.edges then
6:         ADDEDGE(graph, sourceVertex, targetVertex)           ▶ graph library native function
7:       else
8:         if sourceVertex not in graph.vertices then
9:           ADDVERTEX(graph, sourceVertex)                       ▶ graph library native function
10:        if targetVertex not in graph.vertices then
11:          ADDVERTEX(graph, targetVertex)
12:        ADDEDGE(graph, sourceVertex, targetVertex)
13:   return
14: function RUNGROW(subGraph, add)
15:   if add then                                                 ▶ add subGraph into graph
16:     ADDSUBGRAPH(subGraph)
17:   UPDATEMETADATA(subGraph)                                     ▶ Existing Fluxion function to update scheduler state
18:   return
19: function MATCHGROW(jobSpec)
20:   subGraph ← MATCHALLOCATE(jobSpec)
21:   if subGraph then                                           ▶ resources found locally
22:     RUNGROW(subGraph, false)
23:   else                                                         ▶ subGraph = ∅
24:     parent ← GETPARENT()
25:     if parent = ∅ then                                         ▶ top level
26:       if #EXTERNALAPI then
27:         return ∅
28:       subGraph ← EXTERNALAPI(jobSpec)
29:     else
30:       subGraph ← REMOTEPROCEDURECALL(parent, MATCHGROW(jobSpec))
31:     RUNGROW(subGraph, true)
32:   return subGraph

```

across Mellanox QDR HCAs via IP over InfiniBand (IPoIB). We populate test graphs with the configurations detailed in Table 2 with a tree topology, and the test jobspecs are described in Table 1. We use the default Fluxion settings except for the pruning filter setting, for which we use ALL : core, because it ensures better graph search pruning for our tests. We test KubeFlux on a 26 node OpenShift cluster at IBM T.J. Watson research center. Each node contains 2 sockets with 10 Power8™ per socket and SMT8 for a total 160 cores per node, 4 Tesla K80 GPUs, and 512 GB memory.

5.1 Single-level overhead

We first evaluate the performance and memory overheads at the single-scheduler level. We employ resource-query, a Fluxion utility for scheduler testing and reporting resource graph and job allocation statistics. We run our tests on a single node, starting one resource-query process at a time.

To establish a comparison between MATCHGROW (MG) and MATCHALLOCATE (MA) (Sec. 3), we test two different resource graphs. The baseline test configuration begins by initializing a resource graph of 143 vertices and edges (L3 in Table 2). The test issues two MA calls with each jobspec corresponding to T7 in Table 1.

The MG test configuration initializes a subgraph of 73 vertices (L4 in Table 2) and edges and issues a MA requesting all resources (one node with two sockets and 32 cores). Once satisfied, the test executes an MG requesting a subgraph corresponding to T7. When the subgraph is added into the local resource graph, the second test’s resource graph contains the same vertices and edges as the first, but has a single allocated job. For each test, resource-query reports the max Resident Set Size (RSS) after initialization and before test finalization. We also record the elapsed time of MA and MG. We repeat each test 100 times and compute the average timings. The results indicate that the average match times for both tests are approximately equivalent (0.002871s for MA versus 0.002883s for MG), but the subgraph update procedure takes 0.005592s on average for MG (MA does not require the update). The max RSS values are also comparable (5776kB for MA versus 5840kB for MG), indicating that MG increases memory usage linearly in the subgraph size.

5.2 Nested MATCHGROW

We run nested MG tests on two nodes with a hierarchy of five levels. Each level in the hierarchy populates a resource graph in JGF with identical Fluxion scheduling options. Concretely, L0 is

run on physical node0, and reads a JGF to populate a simulated cluster-level resource graph consisting of 18,061 vertices and edges. Level1 along with levels two through four reside on node1, which is configured identically to node0. The deeper nested levels are configured similarly. Table 2 shows each level’s constituents and graph size. The experiments test the timings for each level to issue an RPC and to receive a subgraph in return, perform an MG, add the received subgraph into the local resource graph, and update the scheduler metadata. We perform six tests with successively larger requested subgraph sizes. Subgraph sizes are listed by their number of vertices plus edges. For example, the final test (T8) is a jobspec request of 16 cores on one socket (equivalent to the requests previously allocated at this level during test initialization). See Table 1 for request details.

Table 1: MATCHGROW request tests

Test	nodes	sockets	cores	graph size
T1	64	128	2048	4480
T2	32	64	1024	2240
T3	16	32	512	1120
T4	8	16	256	560
T5	4	8	128	280
T6	2	4	64	140
T7	1	2	32	70
T8	0	1	16	36

Table 2: Graph sizes by level

Level	nodes	sockets	cores	graph size
L0	128	256	4096	18,061
L1	8	16	256	563
L2	4	8	128	283
L3	2	4	64	143
L4	1	2	32	73

After the environment is completely initialized, a helper script starts a test by executing an MG at the leaf (L4), specifying one of the test requests in jobspec format. Levels 1-4 are configured to be fully allocated, so they successively forward the request up the tree until reaching L0. L0 succeeds in matching the resources, and returns them to L1 after updating its scheduler metadata with the new resources allocated to the job. Upon completion of the subgraph add and update steps, the helper script reinitializes the resource graphs at each level and repeats the request. We perform each test 100 times to gather representative data and compute statistics.

5.2.1 Inter-level communication time. A graph-based fully hierarchical scheduler needs to transmit subgraphs between child-parent pairs in linear time with no other dependencies. If a child issues an MG RPC with a particular jobspec and receives the matched resources from its parent, the communication time should only depend on the number of vertices and edges in the matched subgraph.

To measure communication times between child and parent, we record elapsed time between issuing an RPC and receiving the response. Figure 1a shows the distributions of communication times for the T2 test. In the interest of clarity, we limit our presentation to this size, since the other tests’ distributions manifest similarly except for their positions on the vertical axis. In other words, while the tests indicate that communication depends on the subgraph size, the behavior across the tests sizes is similar.

Figure 1a demonstrates that communication time does not depend on resource graph size (implicit in the levels). Levels two through four are very similar: their spread, as seen by the interquartile ranges (IQRs) and whiskers, and medians are nearly identical. However, noting the break in the vertical axis, communication time and behavior does depend on relative location of the parent and child pair. The L1 communication time has a markedly wider IQR, and a much higher median value. Since L1’s parent resides on a remote node, the communication times include internode communication, which we expect to be slower than intranode (as seen with levels two through four). We build linear regression models for inter- and intranode communications and evaluate them based on timing data, and conclude that the times depend on the request size.

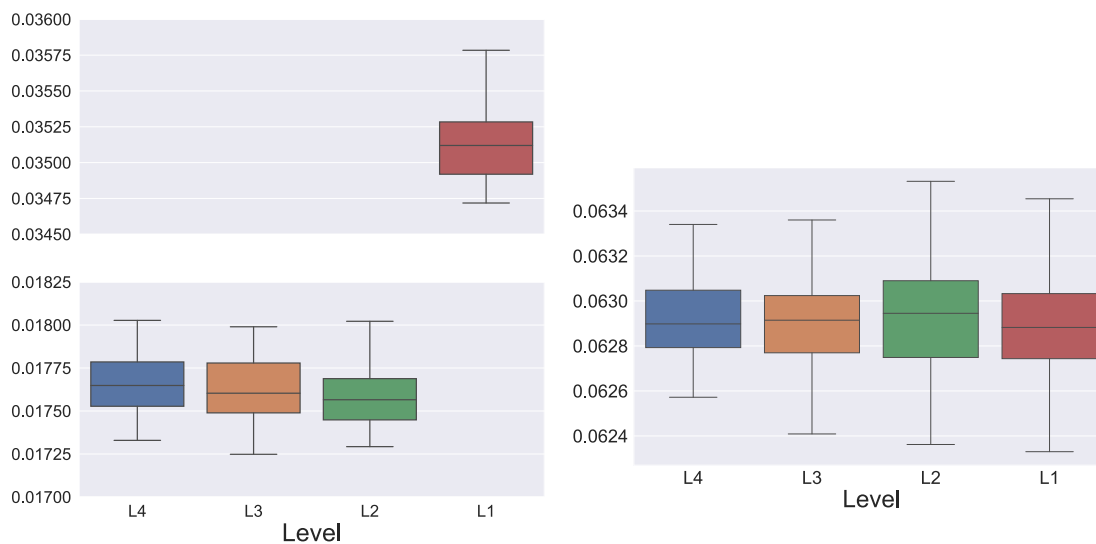
5.2.2 Subgraph update time. For a resource graph with a tree topology, add and update stages necessitate an addition operation for each subgraph vertex and edge, and then a depth-first traversal of the new subgraph to update metadata (see Section 3). In Fluxion, the traversal can be pruned because all previous resource vertices are allocated, so only the newly added subgraph needs to be explored. The add and update stages should only depend on the subgraph size and the number of ancestors of the subgraph root.

We measure the time taken to perform the add and update stages within the overall MG operation. Figure 1b shows the distributions of results for the T2 test. Like the communication time tests, the add-update tests exhibit similar behavior across test sizes; in the interest of clarity we only present one size here. The boxplots indicate no dependence on the level’s resource graph size since there are no clear differences between the IQRs and medians relative positions (e.g. non-overlapping).

5.2.3 Resource match time. The final measurement collected during each test is the time for each level to attempt to find resources matching the request. For an abstract graph-based RJMS, we expect the complexity to be $O(n+m)$ for a resource graph of $n+m$ vertices and edges. However, as Fluxion employs pruning filters, which prevent traversal into allocated subtrees, the complexity is less. In particular, we expect to see complexity dependent on the number of high-level resources (higher than core, at least) in the resource graph. The results of mean match times across all test sizes for levels one through four indicate a small dependence on resource graph size within a test but, there is no obvious dependence on request subgraph size. Level one exhibits different behavior as it finds successful matches. For a successful match, there is a complicated dependence on the request subgraph size and topology which is due to the relationship between the pruning filters used and the configured level of detail in the resource graph [15]. Exploring the performance of successful matches is not our goal in this work.

5.3 Bursting to EC2

In this section, we test whether a graph-based RJMS can effectively request and create cloud resources within a reasonable amount of time. We also compare the static resource configuration used by a traditional bitmap-based scheduler to the Fluxion dynamic resource model by bursting tests to Amazon EC2 Fleet. We choose AWS EC2 and EC2 Fleet for external resource testing due to their rich APIs



(a) Measured communication timing distributions for test T2, or subgraph size 2240. Each boxplot consists of 100 communication timing measurements. Levels 2-4 manifest very similarly, with overlapping IQRs and nearly equivalent medians. However, level 1 is distinct: its spread is larger, and the median value is larger. Its behavior is different from the deeper nested levels.

(b) Measured add and update timing distributions for T2, or subgraph size 2240. Each boxplot consists of 100 add and update timing measurements. All levels manifest very similarly, with overlapping IQRs and nearly equivalent medians.

Figure 1: MATCHGROW overheads

and tremendous request flexibility. In our first test we measure the time necessary to request specific instances from EC2 and receive a response, and the time taken by the Fluxion EC2API plugin to encode the response objects into a JGF subgraph. To do so, a script issues MG from within Fluxion running on a node of our dedicated cluster. We configure EC2API to support eight different instance types and measure the time to request and transform one, two, four, and eight instances at once. We repeat the test 20 times per instance type and request size, totaling 640 tests. The time needed for EC2 to satisfy instance creation requests is effectively constant for all instance types and request sizes up to eight simultaneous instances. See Figure 2 for measured EC2 instance creation time aggregated by instance type. The time to map a Fluxion jobspec to an EC2 instance creation request, as it requires much less than 1% of the instance creation time. The EC2 plugin requires an average overhead to generate JGFs from instance objects of 1.6% of the time needed to create instances.

To demonstrate the flexibility of dynamic resource binding, we compare Fluxion and the EC2API with Slurm’s static binding through EC2 Fleet requests. EC2 Fleet enables requests for sets of instance types, including On-Demand and Spot instances. AWS processes the user request specification and returns a set of instances that meet the constraints. In general, the user does not know which instance types will meet the request or their locations, which is readily accommodated by dynamic binding. Fluxion is capable of adding any combination of instances and their locations into its directed graph at runtime, so Fleets are requested via appropriate

AWS API calls in EC2API. As a simple test, we made 10 Fleet requests of 10 instances each, which took an average of 6.24 seconds from request to the successful addition of the subgraph (44 vertices and edges each) into Fluxion. Note that we allowed AWS to return any of 300 instance types, since the AWS API returns an error if all 349 are specified.

Slurm does not support EC2 Fleet, and its reliance on static binding results in an unmanageable configuration. Encoding EC2 instance types (300 for comparison with Fluxion) and locations (77 current Availability Zones) yields 23,100 node types in the Slurm configuration. Furthermore, bursting to multiple instances of the same type requires a range of instances per type in a partition. Configuring 128 instances per node type as given in the Cloud Scheduling Guide [5] results in a partition with 2,958,600 nodes. To simulate how Slurm handles such a configuration file, we start `slurmctld` and `slurmd` on an LLNL HPC compute node with the file specified. `Slurmctld` and `slurmd` consume 100% CPU each and time out for user input (e.g. `sinfo`) until the daemons are killed by the debug queue one hour walltime.

IBM Spectrum LSF Resource Connector is a highly adaptable interface for LSF, and supports specific Amazon EC2 instance requests as well as bursting to Fleet. Like Fluxion and EC2API, the Resource Connector can integrate any EC2 instance types returned by Spot Fleet, but unlike Fluxion it does not support On-Demand Fleets. Fluxion can make scheduling decisions based on Availability Zones returned by Fleet. However, based on Resource Connector documentation it is unlikely LSF can further enforce global constraints on dynamically provisioned resources (e.g., scheduling hosts from a

specific number of zones and racks) unless it uses a graph resource representation similar to our proposed solution. We cannot make further determinations because this is vendor proprietary information. Furthermore, the Resource Connector exhibits static mapping of cluster users to AWS users, so allowing new users to burst to EC2 requires reconfiguring the user mappings in the connector. Fluxion can avoid this problem by using fully hierarchical scheduling, where a nested Fluxion scheduler can use EC2API as a specific AWS user. See Table 3 for details on the instance configurations and equivalent subgraph sizes.

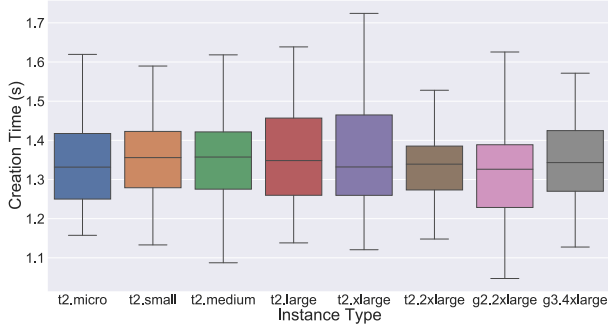


Figure 2: Boxplots of EC2 creation times

The vertical axis designates the time taken for AWS to satisfy a request test by returning a list of instance objects corresponding to the API request. Each box plot aggregates the results from 1, 2, 4, and 8 simultaneous instance requests of each type. Therefore, each boxplot contains 80 test results.

5.4 KubeFlux

Finally, we tested KubeFlux (see Section 2.2) performance on an OpenShift cluster as described above. KubeFlux is composed of three main parts: 1) Fluxion management level, 2) Fluxion daemons (FluxRQ), and 3) the resource graph. The management level collect information to build the resource graph, listens to new scheduling requests, creates job requests to submit to FluxRQ instances, and defines how the resource graph is partitioned among FluxRQ instances. With a new scheduling request, the management level sends a message containing jobspec to a FluxRQ instance. FluxRQs pods run gRPC servers, which wait for pod binding requests on the partition of the Kubernetes cluster described in their resource graph. Upon receiving a binding request, FluxRQs build the Fluxion jobspec in YAML format and submits a MA allocation query to get the target node for pod binding. As part of this effort, we extended KubeFlux so that it can make requests to add and remove resources using MG. The test resource graph contains 4344 vertices and 8686 edges. We evaluate MA and MG when deploying a Kubernetes ReplicaSet with a single pod first, and then scale it up to 100 pods. The MA request is executed once for the first pod allocation, and the average execution time is 0.101810s, while the average execution time for MG requests is 0.100299s.

6 ANALYSIS AND MODELING

In Section 5 we asserted that the time to complete a child-initiated MATCHGROW can be described by the combination of three components: the time to locate resources, the time to communicate

the resource request to the parent Fluxion instance and receive a new subgraph in response, and the time to add the new subgraph into the local instance’s resource graph and update its job metadata. As each of the components is independent of the others, the overall behavior of MATCHGROW is described simply by the sum of the independent components over n levels, i.e. $t_{MG} = \sum_{i=0}^{n-1} t_{match_i} + t_{comms_i} + t_{add_upd_i}$.

Timing data collected in the experiments described in Section 5 supports our assertion. The sum of the three MATCHGROW components at levels one through four accounts for 99.8% of the total measured elapsed time for these levels. Level zero is a special case as it does not include the t_{comms} component, and it emits the matched resources in JGF. Since we do not measure the time to emit the matching subgraph, on average t_{match_0} accounts for 96.4% of the total level time. Across all levels, $t_{match} + t_{comms} + t_{add_upd}$ accounts for 98.2% of the measured time, so we proceed with the confidence that by modeling each component we account for the vast majority of total observed MATCHGROW runtime. With sufficiently accurate component models, we have a sufficiently accurate aggregate model of MATCHGROW behavior.

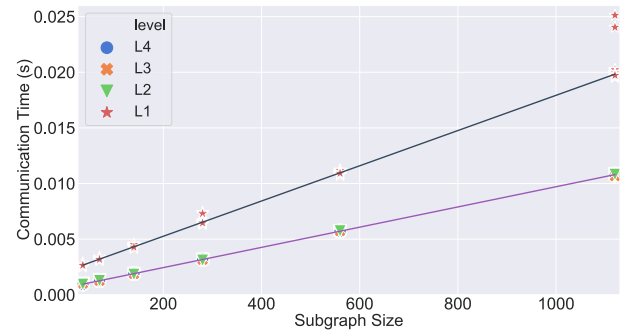


Figure 3: Inter-level communications times by subgraph request size. The horizontal axis indicates the size of the subgraph requested, and the vertical axis indicates the time to communicate the request to each level’s parent via RPC and receive the response as a JGF. Note levels 2-4 obey a different underlying model than level 1; the behavior is due to the different inter-level communications. The regression models are plotted as well to give an indication of the models’ performance.

6.1 Communications model

Recall from Section 5.2.1 that the inter-level communication time should have a linear dependence on the number of vertices plus the number of edges (n) in the subgraph transmitted between levels. Figure 1a indicates that there are two such linear models: one for internode subgraph communication, and one for intranode subgraph communication: $t_{inter} = n\beta_{inter} + \beta_{0inter}$, and $t_{intra} = n\beta_{intra} + \beta_{0intra}$. We have two regression models that we validate with a typical five-fold cross-validation. To develop the models and perform the cross validation, we use the popular Python package Scikit-learn [19]. We report Mean Absolute Percentage Error (MAPE) values, which is a standard choice of interpretable error, and the R^2 value. Table 4

Table 3: EC2 request tests

instance type	CPUs	memory (GB)	GPUs	subgraph size
t2.micro	1	1	0	6
t2.small	1	2	0	8
t2.medium	2	4	0	14
t2.large	2	8	0	22
t2.xlarge	4	16	0	42
t2.2xlarge	8	32	0	82
g2.2xlarge	8	15	1	42
g3.4xlarge	16	128	4	282

lists the MAPE and R^2 values averaged across the five cross validation tests, and the regression coefficients obtained by fitting all data. Both the inter and intranode models fit the data very well, with small average MAPEs and high R^2 values. Taken together the metrics provide strong evidence that the linear models represent the data without omitting independent variables.

Figure 3 is a plot of the two regression models with data included, and is complementary to Figure 1a. The vertical axis indicates the time to communicate the request to each level’s parent via RPC and receive the response as a JGF. The horizontal axis indicates the size of the subgraph requested. The plot provides visible confirmation for the excellent model fits, and indicates the different β_0 coefficients returned by regression. The β_0 coefficients represent the time needed to transmit a subgraph of zero vertices and edges, which can be considered the communication initialization time. The β coefficients, or slopes, represent the bandwidth of each model. If we tested transmission of much larger subgraphs (millions of vertices and edges), we would expect the two models to diverge in terms of bandwidth: the intranode bandwidth should exceed the internode bandwidth as IPoIB becomes a bottleneck. To apply these models, we must know whether a parent and child communicate locally or remotely. However, we assume we are free to choose the Fluxion job hierarchy which holds whenever a user controls its placement.

6.2 Add-update model

In Section 5.2.2 we contended that the time to add a new subgraph and update the metadata in a level’s local resource graph is linearly dependent on the number of vertices and edges (n) in the subgraph. Here we adopt our strategy from the previous section and posit a linear model: $t_{add_upd} = \beta n + \beta_0$. As before, we validate the linear regression with five-fold cross validation. Table 4 includes the average (across the five cross validation tests) MAPE and R^2 values. The linear model exhibits a low error and high R^2 like the communication models, indicating that it represents the data with high fidelity and without omitting variables. Note that the intercept in Table 4 is exactly zero. The Scikit-learn regression model returns a small negative (thus unphysical) value, so we set the intercept to zero to obtain the coefficients in the table. Figure 4 provides a visual representation of the excellent fit of the linear model to the data. It also highlights the small spread and comparable medians of the measurements across different levels, providing a more comprehensive view of Figure 1b.

6.3 Match model

Figure 1b in Section 5.2.2 demonstrates that the time to return a null match depends on the resource graph size, but not the request subgraph size for the jobspecs in the test. In general, however, an arbitrarily complicated jobspec will require more time to return a null match than one with simple core and node requirements. Furthermore, for a request with matching resources, there is a complicated dependence on the request subgraph size and topology. The behavior is due to the relationship between the pruning filters used and the configured level of detail in the resource graph [15]. Instead of embarking upon an in-depth study of the performance space of resource graph size and topology, and request graph size and topology (which is not our goal in this work), in this section we derive an upper bound for the time needed to find matching resources. Such an upper bound provides insight into the scalability of the nested MATCHGROW procedure.

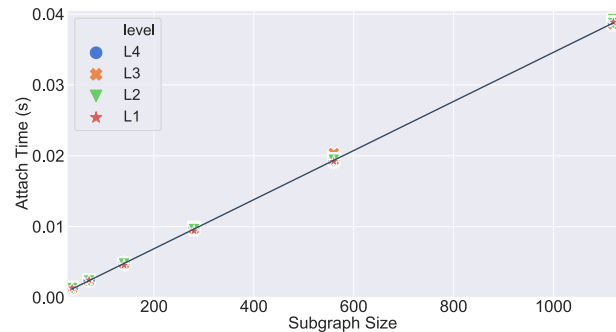


Figure 4: Subgraph add/update times by subgraph request size. The horizontal axis indicates the size of the subgraph to be added, and the vertical axis indicates the time to add the subgraph into each level’s resource graph and then update the resource graph’s scheduling data. The regression models are plotted as well to give an indication of the models’ performance.

Let b be the minimum branching factor between levels in a nested Fluxion job represented by a balanced tree with $b > 1$. Let $s_0 = |V| + |E|$, where $G_0 = (V, E)$ is the top-level resource graph (level 0). Assume the time for Fluxion to complete a MATCHGROW for a fixed request size on a single level is linear in the sum of graph vertices and edges x , i.e.: $\beta x + \beta_0$.

Table 4: Regression model cross validation results and coefficients to five significant digits

model	CV results		reg coefs	
	avg MAPE	avg R^2	β	β_0
L0 comm	0.0090208	0.99774	1.5829×10^{-5}	0.0020992
L1-4 comm	0.0027139	0.99990	9.0824×10^{-6}	0.00063196
attach	0.0088698	0.99991	3.4583×10^{-5}	0.0

Now we want to derive a loose upper bound for the time to complete a match allocate for all levels. To do so, we make a conservative assumption that the linear model can be applied at each level, regardless of whether the level finds a match (which it does not). In fact the time to return a null match is much less. Then the time to complete a MATCHGROW at level 0 is $t_0 = \beta s_0 + \beta_0 \implies t_0 > \beta s_0$ since $\beta_0 > 0$ (it must take positive time for a null resource graph). Then at some level m , $t_0 b^{-m} > \beta s_0 b^{-m}$ so the sum of the first term over all nested levels is:

$$\sum_{k=0}^{\log_b s_0 - 1} t_0 b^{-k} > \sum_{k=0}^{\log_b s_0 - 1} \beta s_0 b^{-k} \quad (3)$$

Where $\log_b s_0$ is the maximum number of levels for a graph of size and order s_0 with branching factor b . Now applying the Geometric Sum Formula to the left hand side yields:

$$\begin{aligned} \sum_{k=0}^{\log_b s_0 - 1} t_0 b^{-k} &= t_0 \left(\frac{1 - b^{-\log_b s_0}}{1 - b^{-1}} \right) \\ &= t_0 b \left(\frac{1 - \frac{1}{s_0}}{b - 1} \right) \end{aligned} \quad (4)$$

And adding the intercept term back in $\log_b s_0$ times gives an upper bound for the total time:

$$t_0 b \left(\frac{1 - \frac{1}{s_0}}{b - 1} \right) + \beta_0 \log_b s_0 > \sum_{k=0}^{\log_b s_0 - 1} \beta s_0 b^{-k} + \beta_0 \quad (5)$$

Which for large s_0 , $t_0 \gg \beta_0$, and $b = 2$ (which is approximately the case in our experiments; see Section 5.2) is $\approx 2t_0$. Note that β_0 is the time needed to return a null match for a null resource graph, so our assumption above is justified. With such a bound in place, we just need to know how long it takes to perform MATCHGROW at a single level with sufficient resources, which is nearly identical to a MATCHALLOCATE (see Algorithm 1).

6.4 Applying the model

In the previous sections we develop components models for each of $t_{match} + t_{comms} + t_{add_upd}$. The full model can be written (to three significant digits) as:

$$\begin{aligned} t_{MG} &= 2t_0 + m(1.58 \times 10^{-5}n + 0.00210) \\ &+ p(9.08 \times 10^{-6}n + 0.000632) + qn3.46 \times 10^{-5} \end{aligned} \quad (6)$$

Where n is the sum of vertices and edges in the subgraph request, m is the number of parent-child levels communicating via IPoB, p is the number of local parent-child pairs, and q is the number of nested levels. In our experiments from Section 5 the values are: $m = 1$, $p = 3$, $q = 4$. To evaluate our model, we use a jobspec requesting multiple node-local resources and compare our model's predicted

time to the observed time. Specifically, the jobspec requests one node with 4 GPUs and two sockets, each with 16 CPUs and 4GB memory. The equivalent subgraph representation is size 94 vertices and edges. Table 5 lists the component model and the corresponding MAPE value. Since the overall model is linear, the total MAPE is just the average of the component errors.

Table 5: Component model prediction accuracy

component model	MAPE
t_{match}	16.106
t_{comms}	0.0039155
t_{add_upd}	0.0077445

The MAPE values in Table 5 for the t_{comms} and t_{add_upd} component models are very low, demonstrating that the models generalize well to a new (and more complex) resource subgraph request. The MAPE value for the t_{match} model is moderate. The loose upper bound derived in Section 6.3 contains several assumptions that guarantee the bound but contribute to its looseness. First, the worst-case assumption that there are $\log_b s_0$ levels translates to 14 levels (for our resource graph of size 18,061) rather than the five present in our tests. Ultimately t_{match} is dominated by the single successful MATCHALLOCATE (unsuccessful calls are much faster) which is approximately the same scenario as a single-level MATCHALLOCATE. As Fluxion has proved to be fast and scalable for single-level MATCHALLOCATE [7] we conclude that it is also fast and scalable for nested MATCHGROW.

7 RELATED WORK

In Prabhakaran et al, 2014 [20] the group proposes a system for dynamically allocating resources to evolving applications. The system balances fairness between rigid and evolving jobs, and is implemented in Maui. Prabhakaran et al, 2018 [22] create a method for dynamic replacement of failed nodes. To do so the method uses Maui to allocate nodes from those in use by malleable applications, or allocates free nodes from a pool of spares. The Slurm resource manager [26] supports expand and shrink operations by allowing a running job to submit a new job with a dependency indicator and then merging the allocations. The approach used by Slurm demands that a job with dynamic resources release all the nodes that came with a single dynamic request. The works by Prabhakaran et al and the Slurm RJMS differ from our study in that the total number of resources does not change; the jobs are elastic, but the clusters are not. Our work enables both forms of dynamism.

Marshall et al, [16] develop an "elastic-site" model that enables on-premise services to use elastically-provisioned cloud resources.

Their model is built on the Nimbus Platform. The main focus of the work is to determine when to burst, rather than how; to that extent the work complements ours. Netto et al, 2018 [18] provide a comprehensive survey of the investigations and remaining challenges related to running HPC applications in the cloud. The suitability of applications for cloud execution is explored in several studies. In particular, Clemente-Castelló et al [9] derive a cost model for cloud bursting MapReduce workflows.

8 CONCLUSIONS

Emerging complex scientific workflows demand extreme, dynamic resource heterogeneity supplied by the latest HPC and cloud converged systems. The massive complexity of the new systems translates to an explosive growth of the resource configuration space, which is becoming unmanageable by current HPC RJMS. We identify three key capabilities needed to manage the configuration space effectively: RJMS elasticity to accommodate elastic jobs, specialization of external resources to manage resources selected by the resource provider, and the capability to schedule cloud orchestration framework tasks. These capabilities have been studied individually, but to the best of our knowledge our work is the first to consider and address all three core capabilities combined. We propose a novel way to provide the capabilities via integrating a dynamic, directed graph-based resource model with fully hierarchical scheduling, and define procedures to edit the resource graph efficiently. We embody the capabilities in Fluxion, a new graph-based RJMS, by imbuing it with resource dynamism and bursting capability. We then run a series of experiments to evaluate the suitability of our solution for managing massive resource configuration spaces. Our results demonstrate that our proposed solution can provide the three key capabilities for managing extreme, dynamic heterogeneity. Our solution lights a beacon for next-generation computing centers that will use abundant elasticity in dynamic workflows and convergence with the cloud.

ACKNOWLEDGMENTS

We are grateful to the entire Flux team for their help addressing test-related issues with software and configurations. In particular, Jim Garlick and Mark Grondona provided invaluable advice with experimental design and optimization, as well as help with diagnostic implementation problems. We wish to thank Jeff Buseman, David Fox, and Robin Goldstone for creating and configuring our test cluster and for enabling our AWS EC2 tests.

This work was performed under the auspices of the U.S. Department of Energy by Lawrence Livermore National Laboratory under Contract DE-AC52-07NA27344 (LLNL-JRNL-826450-DRAFT).

REFERENCES

- [1] 2002. *The Boost Graph Library: User Guide and Reference Manual*. Addison-Wesley Longman Publishing Co., Inc., USA.
- [2] 2021. IBM Spectrum LSF resource connector. https://www.ibm.com/support/knowledgecenter/SSWRJV_10.1.0/lsf_welcome/lsf_kc_resource_connector.html. Retrieved February 10, 2021.
- [3] 2021. Pittsburgh Supercomputing Center Bridges-2 Supercomputer. <https://www.psc.edu/resources/bridges-2/>. Retrieved February 10, 2021.
- [4] 2021. San Diego Supercomputer Center Expanse Supercomputer. <https://www.sdsc.edu/services/hpc/expanse/>. Retrieved February 10, 2021.
- [5] 2021. SchedMD Cloud Scheduling Guide. https://slurm.schedmd.com/elastic_computing.html. Retrieved February 10, 2021.
- [6] 2021. Volcano Kubernetes native batch system. <https://volcano.sh/en/>. Retrieved February 10, 2021.
- [7] Dong H. Ahn et al. 2020. Flux: Overcoming scheduling challenges for exascale workflows. *Future Generation Computer Systems* 110 (2020), 202 – 213.
- [8] Altair Engineering Inc. 2020. *Altair PBS Professional 2020.1 Cloud Guide*. Altair Engineering Inc.
- [9] F. J. Clemente-Castelló, R. Mayo, and J. C. Fernández. 2017. Cost Model and Analysis of Iterative MapReduce Applications for Hybrid Cloud Bursting. In *2017 17th IEEE/ACM International Symposium on Cluster, Cloud and Grid Computing (CCGRID)*. 858–864.
- [10] Francesco Di Natale et al. 2019. A Massively Parallel Infrastructure for Adaptive Multiscale Simulations: Modeling RAS Initiation Pathway for Cancer. In *Proceedings of the International Conference for High Performance Computing, Networking, Storage and Analysis (Denver, Colorado) (SC '19)*. Association for Computing Machinery, New York, NY, USA, Article 57, 16 pages.
- [11] Dror G. Feitelson and Larry Rudolph. 1996. Towards Convergence in Job Schedulers for Parallel Supercomputers. In *Proceedings of the Workshop on Job Scheduling Strategies for Parallel Processing (IPPS '96)*. Springer-Verlag, Berlin, Heidelberg, 1–26.
- [12] A. Gupta, B. Acun, O. Sarood, and L. V. Kalé. 2014. Towards realizing the potential of malleable jobs. In *2014 21st International Conference on High Performance Computing (HiPC)*. 1–10.
- [13] A. Gupta, L. V. Kale, F. Gioachin, V. March, C. H. Suen, B. Lee, P. Faraboschi, R. Kaufmann, and D. Milojicic. 2013. The Who, What, Why, and How of High Performance Computing in the Cloud. In *2013 IEEE 5th International Conference on Cloud Computing Technology and Science*, Vol. 1. 306–314.
- [14] L. V. Kale, S. Kumar, and J. DeSouza. 2002. A Malleable-Job System for Time-shared Parallel Machines. In *2nd IEEE/ACM International Symposium on Cluster Computing and the Grid (CCGRID'02)*. 230–230.
- [15] Lawrence Livermore National Laboratory. 2014. Fluxion. <https://github.com/flux-framework/flux-sched>.
- [16] P. Marshall, K. Keahey, and T. Freeman. 2010. Elastic Site: Using Clouds to Elastically Extend Site Resources. In *2010 10th IEEE/ACM International Conference on Cluster, Cloud and Grid Computing (CCGRID)*. 43–52.
- [17] Amanda J. Minnich et al. 2020. AMPL: A Data-Driven Modeling Pipeline for Drug Discovery. *Journal of Chemical Information and Modeling* 60, 4 (2020), 1955–1968. PMID: 32243153.
- [18] Marco A. S. Netto, Rodrigo N. Calheiros, Eduardo R. Rodrigues, Renato L. F. Cunha, and Rajkumar Buyya. 2018. HPC Cloud for Scientific and Business Applications: Taxonomy, Vision, and Research Challenges. *ACM Comput. Surv.* 51, 1, Article 8 (Jan. 2018), 29 pages.
- [19] F. Pedregosa, G. Varoquaux, A. Gramfort, V. Michel, B. Thirion, O. Grisel, M. Blondel, P. Prettenhofer, R. Weiss, V. Dubourg, J. Vanderplas, A. Passos, D. Courville, M. Brucher, M. Perrot, and E. Duchesnay. 2011. Scikit-learn: Machine Learning in Python. *Journal of Machine Learning Research* 12 (2011), 2825–2830.
- [20] S. Prabhakaran, M. Iqbal, S. Rinke, C. Windisch, and F. Wolf. 2014. A Batch System with Fair Scheduling for Evolving Applications. In *2014 43rd International Conference on Parallel Processing*. 351–360.
- [21] S. Prabhakaran, M. Neumann, S. Rinke, F. Wolf, A. Gupta, and L. V. Kale. 2015. A Batch System with Efficient Adaptive Scheduling for Malleable and Evolving Applications. In *2015 IEEE International Parallel and Distributed Processing Symposium*. 429–438.
- [22] S. Prabhakaran, M. Neumann, and F. Wolf. 2018. Efficient Fault Tolerance Through Dynamic Node Replacement. In *2018 18th IEEE/ACM International Symposium on Cluster, Cloud and Grid Computing (CCGRID)*. 163–172.
- [23] Dan Stanzione, John West, R. Todd Evans, Tommy Minyard, Omar Ghattas, and Dhableswar K. Panda. 2020. Frontera: The Evolution of Leadership Computing at the National Science Foundation. In *Practice and Experience in Advanced Research Computing (Portland, OR, USA) (PEARC '20)*. Association for Computing Machinery, New York, NY, USA, 106–111.
- [24] Jeffrey S. Vetter et al. 2018. Extreme Heterogeneity 2018 - Productive Computational Science in the Era of Extreme Heterogeneity: Report for DOE ASCR Workshop on Extreme Heterogeneity. (12 2018).
- [25] Chih-Chieh Yang, Giacomo Domeniconi, Leili Zhang, and Guojing Cong. 2020. Design of AI-Enhanced Drug Lead Optimization Workflow for HPC and Cloud. In *IEEE International Conference on Big Data*. 5861–5863.
- [26] Andy B. Yoo, Morris A. Jette, and Mark Grondona. 2003. SLURM: Simple Linux Utility for Resource Management. In *Job Scheduling Strategies for Parallel Processing*, Dror Feitelson, Larry Rudolph, and Uwe Schwiegelshohn (Eds.). Springer Berlin Heidelberg, Berlin, Heidelberg, 44–60.